Time-Dependent Convection Induced by Broken Spatial Symmetries

G. Hartung, F. H. Busse, and I. Rehberg
Physikalisches Institut, Universität Bayreuth, 8580 Bayreuth, Germany
(Received 25 September 1990)

It is demonstrated both experimentally and theoretically that broken translational and vertical symmetries of a horizontal convection layer heated from below can lead to a qualitatively new effect, namely, the onset of time-dependent convection. In particular, the behavior of a non-Boussinesq fluid in a layer with sinusoidal variation of the horizontal boundaries is studied near onset.

PACS numbers: 47.25.−c, 47.20.Ky

In the usual approach to the theoretical treatment of a physical problem the most symmetric configuration capturing the physical phenomenon is introduced. While this procedure is necessary and efficient in most cases, symmetries may sometimes restrict the phenomena that can be described. Qualitatively new and unexpected features of the solutions may appear once symmetries are broken. Such is the case of the spatially modulated Rayleigh-Bénard convection considered in this Letter.

Rayleigh-Bénard convection is usually considered for a *horizontally uniform* fluid layer. The effects of small inhomogeneities can be modeled in a first approach by the introduction of sinusoidal modulations of the height of the convection layer or of the temperatures at the boundaries, as has been done theoretically by Kelly and Pal.[1,2] Their analysis predicts a stationary onset of convection in the case of an arbitrary phase shift between the sinusoidal modulations at the lower and upper boundaries. This result agrees with the intuitive concept that inhomogeneities tend to favor a stationary onset. Our experimental observations described in the following demonstrate the unexpected phenomenon of time-dependent convection. This discrepancy can be explained by the idealization of up-down symmetry used in Refs. 1 and 2. Realistic fluids, however, break this symmetry through non-Boussinesq effects and give rise to the qualitatively new effect described in this paper.

A cross section of the cell used in the experiments is shown in Fig. 1. In order to achieve periodic boundary conditions in one of the horizontal dimensions, the cell was constructed as a cylindrical annulus. Two anodized aluminum rings form the upper and lower boundaries. The inner and outer cylindrical boundaries are made out of glass for the optical measurements, and out of Plexiglas for the temperature measurements. The upper copper block is kept at a constant temperature $T=25 \pm 0.01\,^{\circ}\mathrm{C}$ by a thermostatically controlled water bath, while the temperature difference is produced by electric heating of the lower copper ring. The temperature difference was stable within $\pm 0.01\,^{\circ}\mathrm{C}$ and measured by copper-Constantan thermoelements. The mean height h, thickness d, and diameter of the annular fluid channel are 10, 4.5, and 26.65 mm, respectively. A typical variation of height is shown in Fig. 2(a), where also the parameter Δ denoting the phase difference between the modulations of the upper and lower boundaries is defined. The amplitude of the variation scaled by h is $\delta=0.1$.

The amplitude of convection is measured by sixteen thermistors placed at equal distances on the equator of the outer cylindrical wall of the channel [circles t1 to t16 in Fig. 2(a)]. Thermistor t1 is placed above the maximum height of the lower boundary which defines the origin of the coordinate φ around the circumference. To exclude a possible influence on the convection through self-heating of the thermistors, the convection was alternatively detected by means of the shadowgraph method.[3] Parallel light is sent along the axis of the system and reflected in the radial direction by a conical mirror. The light, after passing through the annular channel and being refracted by the density gradients of the convecting fluid, is detected by sixteen diodes arranged equidistantly (6° angular separation) on a quarter circle. Their locations are indicated in Fig. 2(a) by vertical bars. The positions of the leftmost and rightmost diodes will be re-

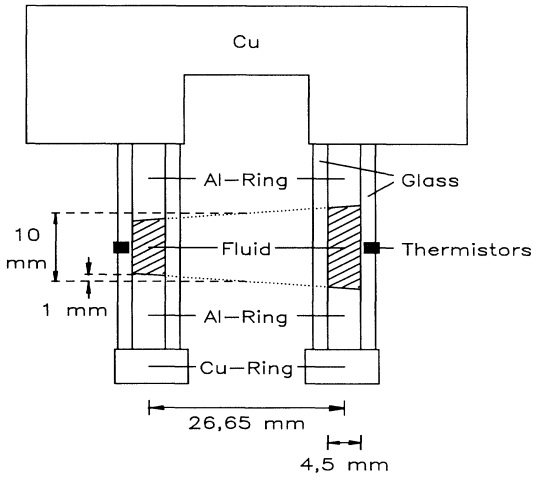

FIG. 1. Cross section of the convection apparatus. The domain of the convecting fluid is hatched.

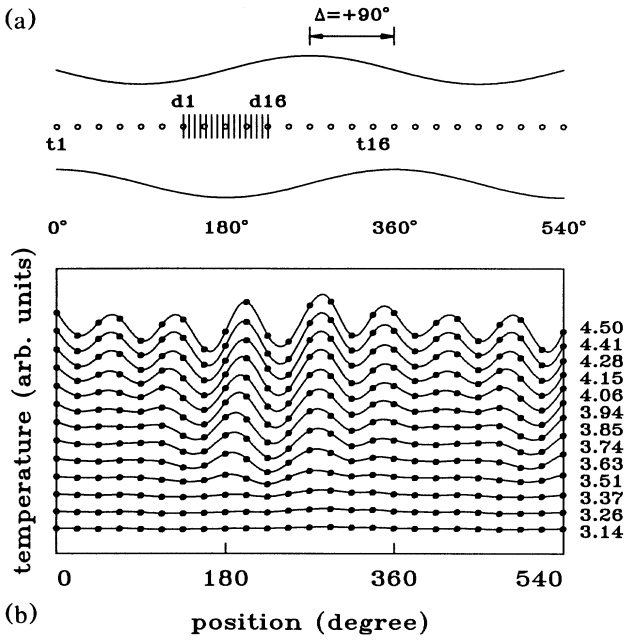

FIG. 2. (a) Positions of the sixteen thermistors (t1–t16, circles) and of the sixteen diodes (d1–d16, vertical bars) in relation to the angle φ (values given at the bottom), and the phase shift angle Δ. The position of the diode array indicated in the figure was used for the measurement displayed in Fig. 3(b). (b) Onset of convection for $\Delta=+90°$. The numbers at the right-hand side are the applied temperature differences. The abscissa gives the angle φ measured in degrees. The data for the interval $0° < \varphi < 180°$ have been repeated for $360° < \varphi < 540°$.

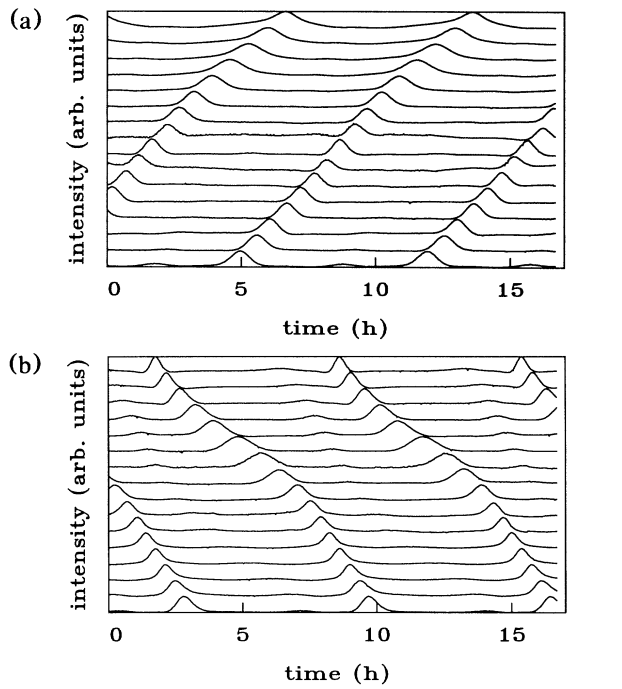

FIG. 3. The light intensity detected by the diodes as a function of time. A maximum of intensity corresponds to downward-flowing fluid in the channel. The lowest line corresponds to diode d1, and the highest line to diode d16. (a) $\Delta=-90°$, $R=4.2R_{c,\mathrm{exp}}$, diode d1 at $\varphi=180°$, diode d16 at $\varphi=270°$. (b) $\Delta=+90°$, $R=4.1R_{c,\mathrm{exp}}$, diode d1 at $\varphi=135°$, diode d16 at $\varphi=225°$.

ferred to by d1 and d16, respectively.

In order to realize the broken up-down symmetry, we use olive oil which has a strong temperature-dependent viscosity (50% variation for the temperature differences used) and is often used to study the influence of this non-Boussinesq effect.

The onset of convection is demonstrated in Fig. 2(b), which displays the thermistor data. Figure 2(a) shows the corresponding variation of the boundaries. To obtain optimal sensitivity, the thermistor signal at a temperature difference below the critical value has been subtracted from the measured signal. The lines through the data are obtained by a Fourier-series interpolation. As must be expected, convection is first detected around $\varphi=225°$ where the maximum height of the channel is located [see Fig. 2(a)]. With increasing ΔT, which is proportional to the Rayleigh number R, the entire channel becomes filled with convection rolls. Although the ratio of circumference to height of the channel is about 8, five pairs of rolls appear. This fact is caused by the finite heat conductivity of the cylindrical side walls which leads to an increase of the critical wave number.[4]

At low Rayleigh numbers R near the critical value when convection occurs primarily in the deeper parts of the channel no time dependence has been observed under stationary conditions. At higher values of R a drift of these rolls starts, as shown in Fig. 3 for two opposite values of the phase shift, $\Delta=-90°$ and $+90°$. The data of this and all following figures were obtained with the diodes. Because of the higher thermal conductivity of glass compared to Plexiglas, R_c is shifted to a higher value in this case.[4] The drift direction always reverses with the sign of the phase shift Δ. The velocity as a function of Δ for a fixed R is shown in Fig. 4. The theory predicts a variation proportional to $\sin\Delta$. Since the measurements were performed at a Rayleigh number much higher than the critical value, deviations from this behavior must be expected. Nevertheless, the theory shows semiquantitative agreement with the experimental results.

The dependence of the drift velocity on ΔT is shown in Fig. 5. The dashed line describes the result of the theory based on the assumption of adiabatic side walls. Much better agreement between theory and experiment is obtained when the observed critical Rayleigh number R_c is used to rescale the theoretical expression (solid line). Note that no other fit parameters have been used to obtain this line. The increase of R_c with increasing ratio

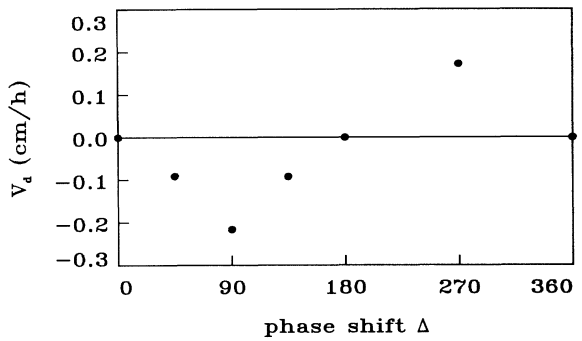

FIG. 4. Measured drift velocity V_d as a function of the phase shift for $R=4.3R_{c,\exp}$.

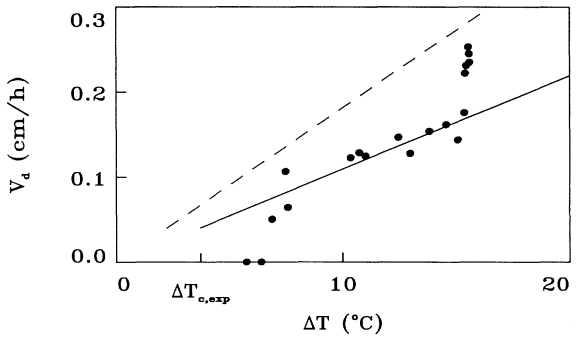

FIG. 5. Drift velocity V_d as a function of temperature difference for $\Delta=-90°$. The circles represent the experimental data and the lines correspond to the theory: For the dashed line the calculated threshold, $\Delta T_{c,\mathrm{th}}=2.23\,°\mathrm{C}$, was used; for the solid line the experimental threshold, $\Delta T_{c,\exp}=3.7\,°\mathrm{C}$, was used.

between side-wall and fluid conductivities agrees approximately with the prediction of an earlier linear theory.[4] The experimental value for R_c was determined by the measurement of the heat transport through the channel. Measurements with the thermistors allowed an independent determination of R_c through the spatial Fourier analysis of the thermistor signals. This method confirmed the heat-transport measurements within the error bars of a few percent. As can be seen from Fig. 5 there exists a range near R_c where no drift is observed even when the entire channel is filled with convection rolls. This property appears to be caused by the highly nonuniform amplitude of the rolls due to the varying height. Such an effect is not included in our theory. Therefore we cannot make a quantitative statement concerning the onset of the drift. With decreasing values of δ this effect will become smaller and the range of validity of the perturbation expansion will increase. For $\delta\rightarrow 0$, the onset of the drift approaches $\varepsilon=0$, although in this limit the drift velocity goes to zero as well. This expectation is supported by preliminary measurements in the case of a smaller δ, which do indeed exhibit the onset of the drift at a smaller value of ε.

The theoretical analysis of the problem is based on a power-series expansion of the dependent variables, e.g., the vertical velocity w, with respect to three small parameters,

$$w=\sum_{\lambda,\mu,\nu}\varepsilon^{\lambda}\gamma^{\mu}\delta^{\nu}w_{\lambda\mu\nu},\quad R=\sum_{\lambda,\mu,\nu}\varepsilon^{\lambda}\gamma^{\mu}\delta^{\nu}R_{\lambda\mu\nu}\,, \tag{1}$$

where ε denotes the amplitude of the convection solution bifurcating from the basic solution of the problem which exhibits the symmetry of the external conditions, and where $\gamma=\hat{\gamma}\Delta T$ measures the change of the dynamic viscosity η between the upper and lower boundaries,

$$\eta=\eta_0[1-\hat{\gamma}(\Theta-z\,\Delta T/h)]\,. \tag{2}$$

In this expression η_0 denotes the viscosity at the mean temperature in the layer and z is the vertical coordinate with the origin on the equatorial plane of the system. Θ describes the deviation of the temperature distribution from the case of pure conduction in the case $\delta=0$. Θ is thus described by an expansion analogous to expansion (1) for w. The summation in (1) starts with zero for all subscripts except that the terms $w_{0\mu 0}$ vanish because the basic solution corresponds to a static equilibrium in the absence of a modulation of the boundaries.

The analysis has been carried to the order $\lambda=\mu=1$, $\nu=2$ and produces the result that a time dependence in the form of a drift is obtained in this order. Since the thermal time scale h^2/κ is relevant for the problem, the order of the drift velocity V_d is thus given by

$$V_d=V\hat{\gamma}\Delta T\,\delta^2\sin\Delta\,\kappa/h\,. \tag{3}$$

V is a complicated integral expression which will be presented elsewhere. In general, V can have either sign depending on the boundary conditions, and turns out to be negative in our case. This is in agreement with the measurements (see Fig. 4). That the drift velocity is proportional to the viscosity contrast of the fluid is confirmed by the linear increase with ΔT observed in the experiment as seen in Fig. 5. The factor δ^2 shows that the drift is produced by a nonlinear quadratic interaction of the components of the basic solution.

In the limit $\gamma\rightarrow 0$ and large aspect ratio d/h, the theory becomes identical to that of Kelly and Pal.[1] Since our theory corresponds to the limit sequence $\delta\rightarrow 0$, $\varepsilon\rightarrow 0$, while the reversed sequence would be appropriate for the description of the experiment near onset, the occurrence of stationary but spatially strongly inhomogeneous convection in the latter regime will require a more complex analysis.

Actual calculations have been carried out only for the case of infinite Prandtl number which is appropriate for our working fluid. Reynolds stresses vanish in this limit and thus do not play a role in generating a mean flow and a resulting drift.[5] Instead an analogous nonlinear term caused by the temperature dependence of the viscosity is responsible for the drift.[5] This can be under-

stood from a consideration of the azimuthal average (indicated by a bar) of the φ component of the Navier-Stokes equations of motion,

$$\eta_0 \nabla^2 \bar{v} = \frac{\eta_0 \gamma}{\Delta T} \left\{ \frac{\partial}{\partial z} \left[\overline{\Theta \left(\frac{\partial}{\partial z} v + \frac{1}{r} \frac{\partial}{\partial \varphi} w \right)} \right] + \frac{1}{r} \frac{\partial}{\partial r} \left[r \left(\overline{\Theta r \frac{\partial}{\partial r} \frac{v}{r}} \right) \right] \right\}. \quad (4)$$

Here the azimuthal velocity component v is separated into its averaged and its fluctuating part, $v = \bar{v} + v$, and r is the radial coordinate. The radial component of the velocity field as well as the radial derivative of Θ have been neglected since they are unimportant in the case of adiabatic side walls. We have also neglected terms of the order γ multiplying $\nabla^2 \bar{v}$ on the left-hand side since they are small in comparison with $\eta_0 \nabla^2 \bar{v}$. From expression (4) it is evident that a mean azimuthal flow $\bar{v}$ is generated in the case of a suitable correlation between v and Θ. As can be shown by a more detailed analysis the mean component $\bar{v}$ of the velocity field does indeed provide the major contribution to the drift rate V_d of the convection pattern.

The experimental results and the theoretical analysis outlined in this paper demonstrate that a small spatial inhomogeneity together with asymmetries may give rise to qualitatively new effects. They are important not only for various applications, but also deserve attention for their underlying mechanism. Since non-Boussinesq properties and small spatial inhomogeneities are typical for naturally occurring convection, the drift effect must be regarded as a universal phenomenon.

The support by the Volkswagenstiftung for the research reported in this paper is gratefully acknowledged.

[1]R. E. Kelly and D. Pal, J. Fluid Mech. **86**, 433 (1978).

[2]D. Pal and R. E. Kelly, in *Thermal Convection with Spatially Periodic Nonuniform Heating: Nonresonant Wavelength Excitation,* Proceedings of the Sixth International Heat Transfer Conference (National Research Council of Canada, Canada, 1978), Vol. 2, p. 235.

[3]S. Rasenat, G. Hartung, B. L. Winkler, and I. Rehberg, Exp. Fluids **7**, 412 (1989).

[4]H. Frick and R. M. Clever, J. Appl. Math. Phys. **31**, 502 (1980).

[5]F. H. Busse, Physica (Amsterdam) **9D**, 287 (1983).